COBEM 2021 26th International Congress of Mechanical Engineering
November 22-26, 2021, Virtual Congress, Brazil
ABCM Associação Brasileira de Engenharia e Ciências Mecânicas

COB-2021-0543
LQR-Backstepping hybrid controller for flight stabilization for autonomous quadrotor

Douglas Luan Cardoso Arena
Magno Enrique Mendoza Meza
Marcos Fernandes Souza
Elvira Rafikova
Federal University of ABC, Graduate Program in Mechanical Engineering- Santo André, Brazil.
douglas.arena@ufabc.edu,br; marcos.fernandes@ufabc.edu.br; magno.meza@ufabc.edu.br; elvira.rafikova@ufabc.edu.br

Abstract. *This article introduces the dynamics of a quadrotor and an hybrid control law designed in a way that the quadrotor trajectory reaches a desired trajectory. The quadrotor dynamics is non-linear, high coupled and underactuated and both control characteristics of the quadrotor flight is a challenge. The proposed control law is based on the application of the linear quadratic regulator (LQR) technique together with the backstepping controller. In order to reduce control efforts, the LQR control technique will be used to obtain virtual controls, they are responsible for determining the control angles, whose objective is to guide the translation movements, resulting in the displacement to the desired positions in x, y e z, and aiming to stabilize and ensure convergence to the desired trajectory, the backstepping control will be responsible for controlling the Euler angles, therefore, it will allow the convergence of angles to the oriented positions ϕ_d e θ_d. The simulation results showed that the LQR-Backstepping control presents satisfactory results in trajectory tracking and with a certain degree of robustness. Thus, it can be concluded that the presented technique is appropriate and effective in the traceability and robustness requirements. The proposed control law is not commonly found in the control literature for application in AUV (quadrotor), therefore, it is intended that the quadrotor flight control area can be expanded with the control law proposed in this work.*
Keywords: *LQR, Backstepping, Quadrotor*

1. INTRODUCTION

Drones are unmanned aerial vehicles (UAVs) that have flight control and receive command signals via radio frequency, infrared or GNSS (Global Navigation Satellite System). The drone, as it is known today, was developed by Israeli space engineer Abraham Karem in 1977, when he arrived in the United States of America (Loureiro, 2017).

UAVs, due to their accessibility and versatility of use, have brought numerous benefits to the UAVs market as well as to consumers. Currently, the UAVs are used for monitoring and surveillance, photo and filming, military use, rescue, etc. The most popular UAVs are fixed wing (similar to an airplane) and rotary wing (similar to helicopters) and multi-rotor (the quadrotor).

In the case of UAVs' four rotor type, their position and attitude are controlled by four rotors and the dynamics are underactuated, strongly coupled and non-linear; also, are influenced by aerodynamic and inertial effects as well as structural vibrations throughout flight. Quadrotors have the ability to perform maneuvers with a high degree of difficulty to avoid obstacles, flight in small spaces, landing and vertical take-offs (Oliveira, 2019). Due to all these characteristics, the quadrotor flight control proves to be a challenge. In the last two decades, there has been a significant growth in the research of quadrotors in the academic and industrial areas; research has been carried out in relation to structure optimization, production cost reduction, computational cost reduction for simulation and development and application of different control techniques (Shi *et al.*, 2019). The problem of driving underactuated UAVs to a desired point with desired orientation attracted the attention of researchers, in the search for control laws in order to achieve exponential and asymptotic stabilization of the system. Therefore, the design of a control law is still an interesting challenge for research (Zain *et al.*, 2015).

In flight control literature, we can find different flight control techniques for quadrotor in order to stabilize and track the desired trajectories. In da Silva Duarte *et al.* (2014), the LQR (Linear Quadratic Regulator) control technique is applied, aiming to control the attitude and translation movements. In Chipofya and Lee (2017), the SDRE control technique was used to track trajectories. In Akgün and Türker (2018), a Backstepping control technique is applied for the control and stabilization of the attitude movements of a quadrirotor. In Sabatino (2015), the feedback-linearization control technique is developed, enabling the convergence of translational movements (x ,y, z) to the desired position.

In this work, we study the four-rotor mathematical model subject to a hybrid LQR-Backstepping control technique, with the purpose of controlling the translational movements (x, y, z). LQR control is an optimization technique that min-

imizes the control effort, and Backstepping control is a technique that recursively uses the concept of Lyapunov functions to determine the control effort. The approach of the present work, in which the LQR technique is applied in combination with the backstepping technique, is not commonly found in the quadrotor flight control literature. This combination of techniques characterizes the novelty of this work.

This work is organized as follows: in section 1 the introduction is presented, in Section 2 the mathematical model of the studied quadrotor is shown, in Section 3 the control techniques used for flight control are presented, in Section 4 the simulations of the system subject to the proposed control technique are shown and finally in Section 5 the conclusions and final considerations are shown.

2. SYSTEM DYNAMICS

In this article, the dynamics studied in Costa (2008) is used. Quadrotor dynamics was obtained using two coordinate systems. One of the coordinates is the system attitude (θ, ϕ, ψ) and the other is the translation coordinate (x, y, z), as shown in Figure 1. The following considerations should be highlighted:

- Quadrotor has a symmetrical structure.
- Quadrotor is a rigid body.
- The center of gravity and the body frame origin are coincided.

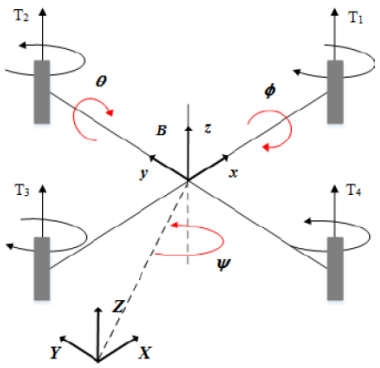

Figure 1: Representation quadrotor.

The rotation dynamics is the representation of the rotation movements ϕ (roll), θ (pitch) and ψ (yaw) is as follows:

$$\ddot{\phi} = \left(\frac{I_{yy} - I_{zz}}{I_{xx}}\right)\dot{\theta}\dot{\psi} + \frac{M_\phi}{I_{xx}} \tag{1}$$

$$\ddot{\theta} = \left(\frac{I_{zz} - I_{xx}}{I_{yy}}\right)\dot{\phi}\dot{\psi} + \frac{M_\theta}{I_{yy}} \tag{2}$$

$$\ddot{\psi} = \left(\frac{I_{xx} - I_{yy}}{I_{zz}}\right)\dot{\phi}\dot{\theta} + \frac{M_\psi}{I_{zz}} \tag{3}$$

The translational dynamics represents linear movements x, y and z is as follows:

$$\ddot{x} = (sin(\phi)sin(\psi) + cos(\phi)cos(\psi)sin(\theta))\frac{T_t}{m} \tag{4}$$

$$\ddot{y} = (cos(\phi)sin(\psi)sin(\theta) - cos(\psi)sin(\phi))\frac{T_t}{m} \tag{5}$$

$$\ddot{z} = -g + (cos(\phi)cos(\theta))\frac{T_t}{m} \tag{6}$$

The state vector is defined as:

$$\mathbf{x} = \begin{bmatrix} x & \dot{x} & y & \dot{y} & z & \dot{z} & \phi & \dot{\phi} & \theta & \dot{\theta} & \psi & \dot{\psi} \end{bmatrix}^T = \begin{bmatrix} x_1 & x_2 & x_3 & x_4 & x_5 & x_6 & x_7 & x_8 & x_9 & x_{10} & x_{11} & x_{12} \end{bmatrix}^T$$

and the controls are:

$$\mathbf{u} = \begin{bmatrix} T_t & M_\phi & M_\theta & M_\psi \end{bmatrix}^T = \begin{bmatrix} U_1 & U_2 & U_3 & U_4 \end{bmatrix}^T$$

3. LQR-BACKSTEPPING HYBRID CONTROL TECHNIQUE

Figure 2 shows the block diagram of the hybrid control technique presented in this section. Note that, the LQR control technique is used for determining the virtual controls, which are responsible for determining the reference angles ϕ_d and θ_d, whose objective is the orientation of the translational movements, resulting in the displacement to the desired positions in x, y and z. The backstepping controller will be responsible for controlling the Euler angles, therefore, it will enable the convergence of the angles to the respective oriented positions (ϕ_d and θ_d), ensuring the evolution of the translation movements to the desired trajectories (x_d, y_d, z_d).

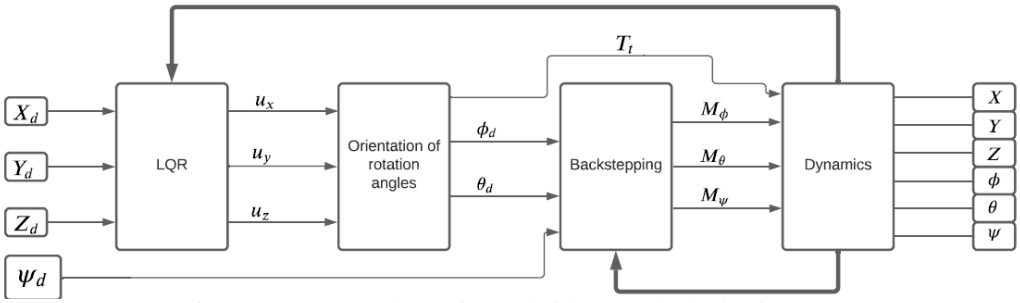

Figure 2: LQR-Backstepping Hybrid Control Block Diagram.

3.1 Control of translational dynamics

According to the proposal in Zuo (2010), virtual controls are used relating them to speeds so that indirectly controlled states can be reached. For the representation, the relationship between the accelerations of the states and virtual controls is determined, according to the following representation:

$$\ddot{x} = u_x, \quad \ddot{y} = u_y, \quad \ddot{z} = u_z.$$

Introducing the dynamics present in equations (4), (5) and (6) in (10), comes to:

$$\ddot{x} = (cos(\psi_d)sen(\theta_d)cos(\phi_d) + sen(\psi_d)sen(\phi_d))\,\frac{T_t}{m} = u_x \tag{7}$$

$$\ddot{y} = (sen(\psi_d)sen(\theta_d)cos(\phi_d) - cos(\psi_d)sen(\phi_d))\,\frac{T_t}{m} = u_y \tag{8}$$

$$\ddot{z} = -g + (cos(\theta_d)cos(\phi_d))\,\frac{T_t}{m} = u_z \tag{9}$$

We assume the simplifying hypothesis that ψ_d = 0, avoiding rotation on the axis z, resulting in algebraic simplifications. Thus, becomes:

$$u_x = sen(\theta_d)cos(\phi_d)\frac{T_t}{m} \qquad u_y = -sen(\phi_d)\frac{T_t}{m} \qquad u_z = -g + (cos(\theta_d)cos(\phi_d))\,\frac{T_t}{m} \tag{10}$$

From the equation (10), becomes:

$$T_t = \frac{m(u_z + g)}{cos(\theta_d)cos(\phi_d)} \qquad \phi_d = arctg\left(-\frac{u_y}{u_z + g}cos(\theta_d)\right) \qquad \theta_d = arctg\left(\frac{u_x}{u_z + g}\right)$$

The LQR will be applied defining a cost function $\mathbf{J}$ to be minimized:

$$\mathbf{J}(\mathbf{x}(t), \mathbf{u}(t)) = \frac{1}{2}\int_0^\infty \left[\mathbf{x}^T(t)\mathbf{Q}\mathbf{x}(t) + \mathbf{u}^T(t)\mathbf{R}\mathbf{u}(t)\right] dt \tag{11}$$

where the matrices $\mathbf{Q}$ and $\mathbf{R}$, weighting matrices, are diagonal matrices and are responsible for the importance given to the state vector and the control action, respectively. The matrix $\mathbf{Q}$ is semi-definite positive symmetric and $\mathbf{R}$ is definite positive symmetric and:

$$\mathbf{x} = \begin{bmatrix} x & \dot{x} & y & \dot{y} & z & \dot{z} \end{bmatrix} = \begin{bmatrix} x_1 & x_2 & x_3 & x_4 & x_5 & x_6 \end{bmatrix},$$

$$\begin{bmatrix} x_d & \dot{x}_d & y_d & \dot{y}_d & z_d & \dot{z}_d \end{bmatrix} = \begin{bmatrix} x_{1_d} & x_{2_d} & x_{3_d} & x_{4_d} & x_{5_d} & x_{6_d} \end{bmatrix}$$

According to Çimen (2008), it is possible to relate the control angles ϕ_d and θ_d and the control input T_t with the virtual controls (u_x, u_y, u_z), these will be determined through the application of the LQR control technique, through the following control law, in order to minimize the cost function (11):

$$\mathbf{u}(t) = -\mathbf{R^{-1}B^{T}P}(t)\mathbf{e}(t) \tag{12}$$

where $\boldsymbol{P}$ is the solution of the following algebraic equation of Riccati, (Voos, 2006), and is unique, symmetric, positive-definite solution:

$$\mathbf{PA} + \mathbf{A^{T}P} - \mathbf{PBR^{-1}B^{T}P} + \mathbf{Q} = 0 \tag{13}$$

and $\mathbf{e}(t)$ is the state vector error:

$$\mathbf{e}(t) = \begin{bmatrix} x_1 - x_{1_d} \\ x_2 - x_{2_d} \\ x_3 - x_{3_d} \\ x_4 - x_{4_d} \\ x_5 - x_{5_d} \\ x_6 - x_{6_d} \end{bmatrix}$$

According to Oliveira (2019), the virtual controls vector is as follows:

$$\mathbf{u}(t) = \begin{bmatrix} u_x & u_y & u_z \end{bmatrix}^T$$

The closed loop dynamics representation is:

$$\dot{\mathbf{x}}(t) = \mathbf{A}\mathbf{x}(t) + \mathbf{B}\mathbf{u}(t) \tag{14}$$

The matrices $\mathbf{R}$ and $\mathbf{Q}$ were obtained by exhaustive search and those that presented the best results are shown as follows:

$$\mathbf{R} = \begin{bmatrix} 1 & 0 & 0 \\ 0 & 1 & 0 \\ 0 & 0 & 1 \end{bmatrix}, \qquad \mathbf{Q} = \begin{bmatrix} 9 & 0 & 0 & 0 & 0 & 0 \\ 0 & 8 & 0 & 0 & 0 & 0 \\ 0 & 0 & 9 & 0 & 0 & 0 \\ 0 & 0 & 0 & 7 & 0 & 0 \\ 0 & 0 & 0 & 0 & 9 & 0 \\ 0 & 0 & 0 & 0 & 0 & 8 \end{bmatrix}$$

Due to the representation of the translational dynamics through virtual controls as presented in the equations (7), (8) and (9), and according to the closed-loop dynamics representation given in the equation (14), the system will be made up of matrices constants $\mathbf{A}$ and $\mathbf{B}$, representing the translational movements of the dynamics, as follows:

$$\mathbf{A} = \begin{bmatrix} 0 & 1 & 0 & 0 & 0 & 0 \\ 0 & 0 & 0 & 0 & 0 & 0 \\ 0 & 0 & 0 & 1 & 0 & 0 \\ 0 & 0 & 0 & 0 & 0 & 0 \\ 0 & 0 & 0 & 0 & 0 & 1 \\ 0 & 0 & 0 & 0 & 0 & 0 \end{bmatrix}, \qquad \mathbf{B} = \begin{bmatrix} 0 & 0 & 0 \\ 1 & 0 & 0 \\ 0 & 0 & 0 \\ 0 & 1 & 0 \\ 0 & 0 & 0 \\ 0 & 0 & 1 \end{bmatrix}$$

3.2 Control of rotation dynamics

The backstepping control is used to carry out the convergence of the rotation dynamics states to the respective desired references (ϕ_d, θ_d and ψ_d). A presentation of the application of the technique for controlling the angle ϕ is show below. The control project starts by changing the variable:

$$e_1 = x_{7d} - x_7 \tag{15}$$

where x_{7d} will be a desired position coordinate and e_1 it is a positional error.

The Lyapunov function is used where the candidate function for the Lyapunov function must be in function of e_1 and must be positive definite and its time derivative must be negative semidefinite (Shi *et al.*, 2019):

$$V_1 = \frac{1}{2}e_1 \tag{16}$$

and time derivative of the equation (16), is:

$$\dot{V}_1 = e_1 \dot{e}_1 \tag{17}$$

The time derivative of the equation (15), $\dot{e_1} = \dot{x}_{7d} - \dot{x}_7$, is introduced into the equation (17), we obtain $\dot{x}_7 = x_8$, rewrite the equation (17) as follows:

$$\dot{V}_1 = e_1(\dot{x}_{7d} - x_8) \tag{18}$$

According to Bouabdallah (2007), it is possible choosing:

$$x_8 = \alpha_1 e_1 + \dot{x}_{7d}; \qquad \text{with} \qquad \alpha_1 > 0; \tag{19}$$

where α_1 is the stabilization constant gain, using the equation (19) into the equation (18), we obtain:

$$\dot{V}_1 = -\alpha_1 e_1^2 \tag{20}$$

From the equation (20) it is observed that $\dot{V}_1$ it will be negative semi-definite, which satisfies the Lyapunov function condition. The second step of the process starts with defining a second Lyapunov function as follows:

$$V_2 = V_1 + \frac{1}{2} e_2^2 \tag{21}$$

The Lyapunov function of the equation (21) is positive definite, the next step will be to derive the equation (21) and ensure that it is negative semi-definite (Nadda and Swarup, 2014):

$$\dot{V}_2 = \dot{e}_1 e_1 + \dot{e}_2 e_2 \tag{22}$$

It is clear that having $e_2 = 0$, we will have $\dot{V}_2 = -\alpha_1 e_1^2$, therefore, we will work on e_2. We will adopt that:

$$e_2 = \dot{x}_{7d} - x_8$$

Considering the previous step, it is decided to adopt that $x_8 = \dot{x}_{7d}$, thus:

$$e_2 = x_8 - \dot{x}_{7d} - \alpha_1 e_1 \tag{23}$$

Deriving the equation (23):

$$\dot{e}_2 = \dot{x}_8 - \ddot{x}_{7d} - \alpha_1 \dot{e}_1$$

Rewriting the equation (22):

$$\dot{V}_2 = -e_1(e_2 + \alpha_1 e_1) + e_2(\dot{x}_8 - \ddot{x}_{7d} - \alpha_1 \dot{e}_1) \tag{24}$$

According to Bouabdallah (2007), it is use the equation (23) so that we eliminate the term $\dot{e}_1$ of the equation (24) :

$$\dot{V}_2 = -e_1(e_2 + \alpha_1 e_1) + e_2(\dot{x}_8 - \ddot{x}_{7d} - \alpha_1(-e_2 - \alpha_1 e_1)) \tag{25}$$

It is introduce the differential equation for the degree of freedom ϕ in the equation (25):

$$\dot{V}_2 = -e_1(e_2 + \alpha_1 e_1) + e_2((a_1 x_{10} x_{12} + b_1 M_\phi) - \ddot{x}_{7d} - \alpha_1(-e_2 - \alpha_1 e_1))$$

Adopting that: a_1 = $((Iyy - Izz)/Ixx)$ e $b_1 = \frac{1}{I_{xx}}$.

It is possible to determine M_ϕ, control input responsible for ensuring that the time derivative of the second Lyapunov function candidate is semi-defined negative, which characterizes that the proposed function is Lyapunov function:

$$M_\phi = \frac{1}{b_1}(-a_1 x_{10} x_{12} - \alpha_1(e_2 + \alpha_1 e_1) + e_1 - \alpha_2 e_2)$$

Remembering that the term $\alpha_2 e_2$ with $\alpha_2 > 0$ is responsible for stabilizing e_1. After this process we obtain:

$$\dot{V}_2 = -\alpha_1 e_1^2 - \alpha_2 e_2^2$$

The concepts regarding Lyapunov functions are satisfied.

Control inputs responsible for controlling rotation angles θ and ψ, are obtained according to the steps shown above to determine M_ϕ. The equations that represent the control inputs are:

$$M_\theta = \frac{1}{b_2}\left(-a_2 x_8 x_{12} - \alpha_3(e_4 + \alpha_3 e_3) + e_3 - \alpha_4 e_4\right)$$
$$M_\psi = \frac{1}{b_3}\left(-a_3 x_8 x_{10} - \alpha_5(e_6 + \alpha_5 e_5) + e_5 - \alpha_6 e_6\right)$$

It is defined that:

$$e_3 = x_{9d} - x_9 \quad \Big| \quad e_4 = x_{10} - \dot{x}_{9d} - \alpha_3 e_3 \quad \Big| \quad a_2 = ((Izz - Ixx)/Iyy) \quad \Big| \quad b_2 = \tfrac{1}{I_{yy}}$$

$$e_5 = x_{11d} - x_{11} \quad \Big| \quad e_6 = x_{12} - \dot{x}_{11d} - \alpha_5 e_5 \quad \Big| \quad a_3 = ((Ixx - Iyy)/Izz) \quad \Big| \quad b_3 = \tfrac{1}{I_{zz}}$$

It has that α_1 ... α_6 are positive constants.

4. NUMERICAL SIMULATION

This section will present the results obtained through numerical simulations, through the application of the fourth order Runge-Kutta numerical method, with integration steps equal to 0.001 s and the initial position is: $[x, y, z, \psi]$ = $[1(m), 1(m), 1(m), 0(rad)]$. The simulation will take place in 3 steps, as follows:

Step1 - In the first 10 seconds, the desired trajectory is defined as:

$$x_d = y_d = z_d = t$$
$$\dot{x}_d = \dot{y}_d = \dot{z}_d = 1 \text{ m/s}$$

Step2 - From the moment $t = 10$ seconds, the desired trajectory is set to be a fixed point, ie:

$$x_d = y_d = z_d = 10$$

Step3 - At time $t = 25$ seconds, the following disturbances were generated and introduced in the system:

$x = 1.10 \times$ current position
$y = 1.05 \times$ current position
$z = 0.90 \times$ current position

In Table 1, the quadrotor parameters used to perform the numerical simulations are presented.

Table 1: Parameter table.

Parameter	Nomenclature	Value
Mass	m	0,650 Kg
Gravity acceleration	g	$9.81 m/s^2$
Moment of inertia on the axis x	I_{xx}	$7,5$ x 10^{-3} $Kg.m^2$
Moment of inertia on the axis y	I_{yy}	$7,5$ x 10^{-3} $Kg.m^2$
Moment of inertia on the axis z	I_{zz}	$1,5$ x 10^{-2} $Kg.m^2$

For the numerical simulation, the stabilization gains were chosen (α_i) that resulted in the best performances, obtained through an exhaustive search:

$$\alpha_1 = 5, \quad \alpha_2 = 2, \quad \alpha_3 = 4, \quad \alpha_4 = 2, \quad \alpha_5 = 1, \quad \alpha_6 = 1.$$

The simulation results of the proposed control system are shown in Figure 3, where the evolution over time of linear positions x, y, z and the angular position ψ, respectively.

In Figure 3, the evolution of the positions can be observed. x, y, z e ψ, and the convergence of states to the desired trajectory occurs approximately after 2 seconds, with an error rate considered negligible after the settlement of the system. From the instant $t = 10$ seconds of simulation, the desired trajectory is fixed. This is interpreted as the quadrotor hovering in a certain position. It is observed that this change in trajectory causes an oversignal in linear positions x, y e z, as can be seen in Figure 3.

In Figure 4, it is observed that at the moment $t = 10$ a sharp deceleration occurs in order to reach the desired trajectory point and at the desired trajectory point, at which the system stabilizes, speeds should reach a null value. The acceleration

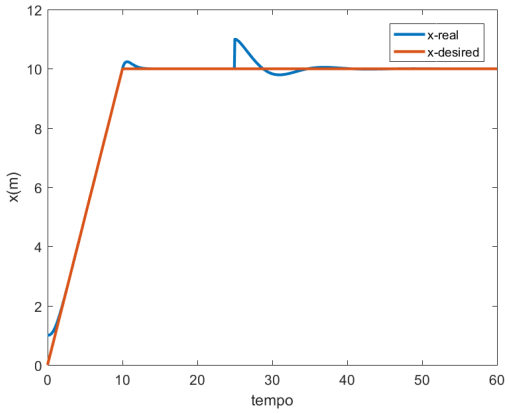

(a) Evolution over time of position x.

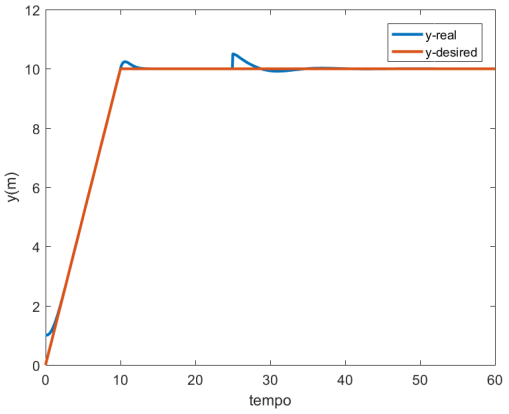

(b) Evolution over time of position y.

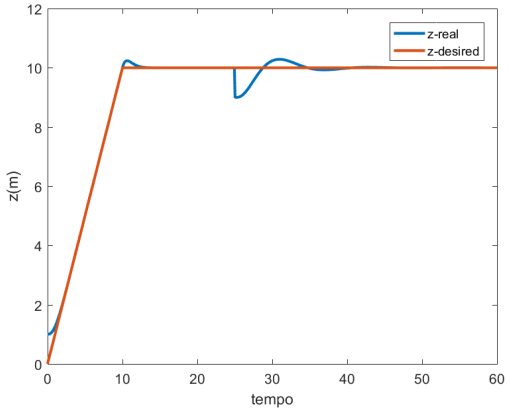

(c) Evolution over time of position z.

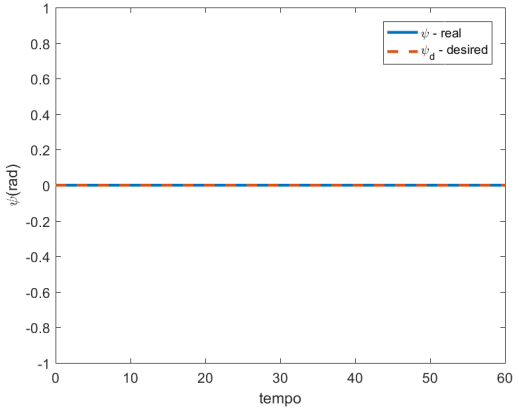

(d) Evolution over time of angular position ψ.

Figure 3: Evolution over time of linear positions and angular position ψ

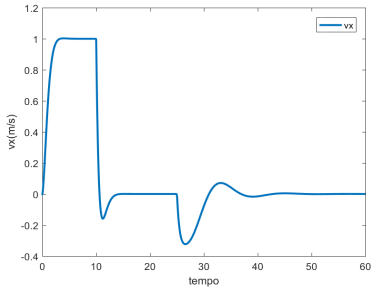

(a) Evolution over time of x speed.

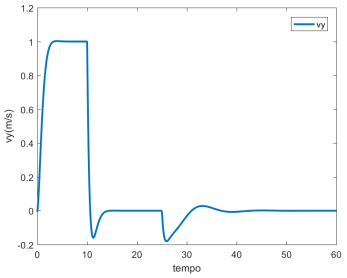

(b) Evolution over time of y speed.

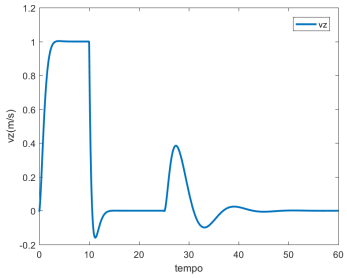

(c) Evolution over time of z speed.

Figure 4: Evolution over time of speeds.

until reaching the desired point and the deceleration occurred after reaching the desired point are responsible for the signals in the positions spare signal x, y and z, in the transition between steps 1 and 2. Even with the presence of these spare signals, the positions return to the desired position, as shown in Figure 3. A perturbation was introduced at the instant $t = 25$ in the respective linear positions, and even with the presence of disturbances, the system returns to the desired trajectory point. This shows that the system stabilized on the desired trajectory and exhibits a certain degree of robustness.

In Figure 5, the representations of the Euler angles are presented ϕ and θ, these being the reference angles, responsible for the orientation of the system, thus enabling the quadrirotor to converge the desired positions in x, y and z. It is noticed that the difference between the achieved angles (ϕ-real and θ-real) and the desired (ϕ_d and θ_d) is despicable.

The representation of the control efforts are presented in Figure 6, where it is possible to analyze the values of the efforts, responsible for generating movement in their respective axes of action. Control input values M_ψ remain null throughout the simulation, as the yaw angle (ψ) movement variation is not required.

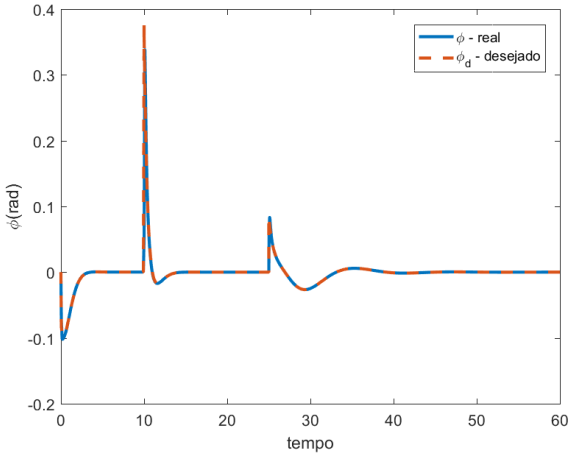

(a) Evolution over time of angular position ϕ.

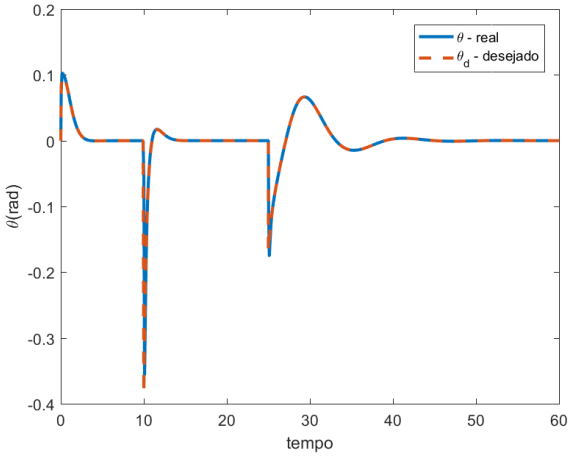

(b) Evolution over time of angular position θ.

Figure 5: Evolution over time of Euler angles.

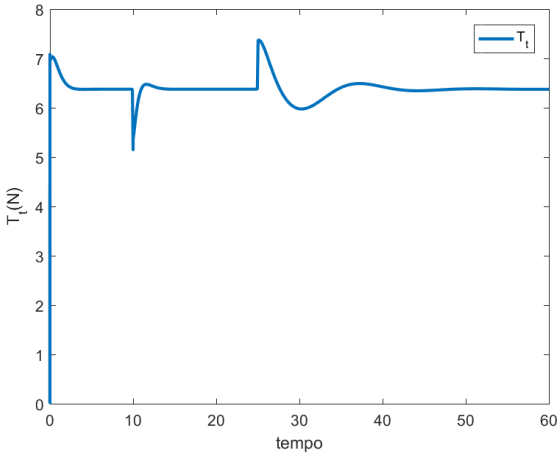

(a) Evolution over time of control effort u_1.

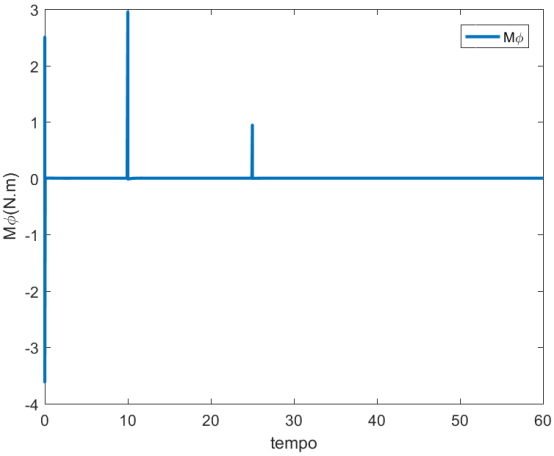

(b) Evolution over time of control effort u_2.

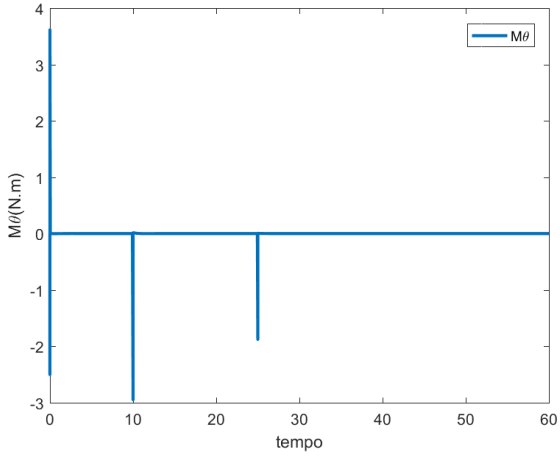

(c) Evolution over time of control effort u_3.

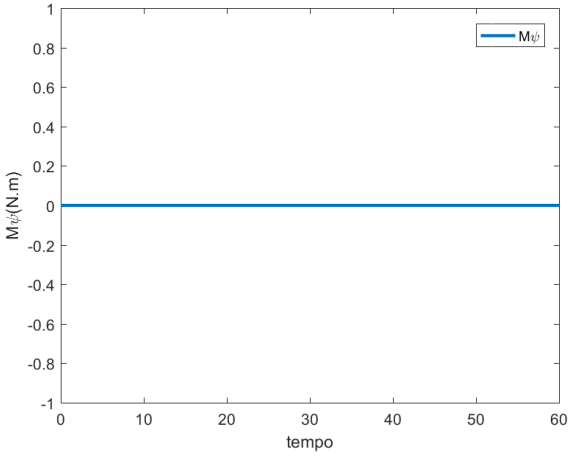

(d) Evolution over time of control effort u_4.

Figure 6: Evolution over time of control efforts.

5. CONCLUSION

The proposed hybrid control shows the following characteristics:

1. An appropriate performance because the system stabilizes in approximately two seconds;

2. The control efforts have reduced values as shown in Figure 6;

3. A certain degree of robustness due to the fact that the system in the presence of disturbances returns to the desired trajectory point and this guarantees that the proposed control can be used in the control of quadrotors flight, although the quadrotors are nonlinear, underactuated and tightly coupled dynamic systems;

4. The proposed control proved to be robust when the system was subjected to disturbances in linear positions, and these disturbances are of the order of 5% and 10% of the value of the desired trajectory point, as can be seen at the instant t = 25 seconds, in Figure 3.

The control law proposed in this work, which consists of the combination of the LQR control and the backstepping control, is not found in the quadrotors control literature. Therefore, it is believed that with the purpose of this article, the area of flight control with quadrotors is being expanded.

The proposed hybrid control will be applied in a prototype of UAVs for heavy load, which is being developed in the Graduate Program in Mechanical Engineering at Federal University of ABC and will be the reason for the elaboration of research articles.

6. ACKNOWLEDGEMENTS

Douglas Arena wishes to acknowledge support given to him from Federal University of ABC through scholarship during all the research period.

7. REFERENCES

Akgün, O. and Türker, T., 2018. "An adaptive block backstepping controller for a quadrotor". In *2018 6th International Conference on Control Engineering & Information Technology (CEIT)*. Ieee, pp. 1–6.

Bouabdallah, S., 2007. *Design and control of quadrotors with application to autonomous flying*. Master's thesis, Ecole Polytechnique federale de Lausanne, Lausanne, Switzerland,ese.

Chipofya, M. and Lee, D.J., 2017. "Position and altitude control of a quadcopter using state-dependent riccati equation (sdre) control". In *2017 17th International Conference on Control, Automation and Systems (ICCAS)*. IEEE, pp. 1242–1244.

Çimen, T., 2008. "State-dependent riccati equation (sdre) control: A survey". *IFAC Proceedings Volumes*, Vol. 41, No. 2, pp. 3761–3775.

Costa, S.E.A.P., 2008. *Control and Simulation of a conventional Quadrirotor*. Master's thesis, Technical University of Lisbon, Portugal. In Portuguese.

da Silva Duarte, M.K., Figueiredo, H. and Saotome, O., 2014. "Análise do rastreador linear quadrático aplicado ao quadricóptero". In *ABCM Symposium Series in Mechatronics*. ABCM, pp. 1124–1133.

Loureiro, J.F.V., 2017. *Sistema autônomo para pouso e recarga da bateria de um ArDrone 2.0*. B.S. thesis, Universidade Tecnológica Federal do Paraná.

Nadda, S. and Swarup, A., 2014. "Development of backstepping based sliding mode control for a quadrotor". In *2014 IEEE 10th International Colloquium on Signal Processing and its Applications*. IEEE, pp. 10–13.

Oliveira, A.C.F., 2019. *Modeling the dynamics and control of an unmanned aerial vehicle of the quadrotor type*. Master's thesis, Federal University of ABC, Brazil. In Portuguese.

Sabatino, F., 2015. "Quadrotor control: modeling, nonlinearcontrol design, and simulation".

Shi, X., Cheng, Y., Yin, C., Dadras, S. and Huang, X., 2019. "Design of fractional-order backstepping sliding mode control for quadrotor uav". *Asian Journal of Control*, Vol. 21, No. 1, pp. 156–171.

Voos, H., 2006. "Nonlinear state-dependent riccati equation control of a quadrotor uav". In *2006 IEEE International Symposium on Intelligent Control*. IEEE, pp. 2547–2552.

Zain, Z.M., Harun, N., Watanabe, K. and Nagai, I., 2015. "Comparison of an x4-auv performance using a direct lyapunov—pd controller and backstepping approach". In *2015 10th Asian Control Conference (ASCC)*. IEEE, pp. 1–6.

Zuo, Z., 2010. "Trajectory tracking control design with command-filtered compensation for a quadrotor". *IET control theory & applications*, Vol. 4, No. 11, pp. 2343–2355.